Dynamical Systems in Robot Control Architectures: A Building Block Perspective

João Sequeira
Instituto Superior Técnico,
Institute for Systems and Robotics,
Lisbon, Portugal, Email: joao.silva.sequeira@ist.utl.pt

Cristina Santos, Jorge Silva
Universidade do Minho, Portugal,
Email: {cristina, jbruno}@dei.uminho.pt

***Abstract*—The paper reviews a known robot control architecture using nonlinear analysis and control theory viewpoints. The architecture is based on a mesh of dynamic systems and feedthrough maps and is able to drive the robot under temporal constraints.**

The analysis points to an intuitive, though innovative, conclusion that control architectures can be constructed from a methodological perspective by mixing (i) dynamical systems with fixed points carefully selected to match mission requirements, and (ii) feedthrough maps that perform memoryless transformations on input data.

Experiments using the Webots environment are presented to illustrate the ideas developed.

I. Introduction

In general, robotic systems can be represented by a mesh of blocks either partially or fully interconnected. Typical examples of such blocks are the localization systems, and sensor acquisition and processing. The information exchange among the blocks is often of heterogeneous types and each of them will evolve in time according to some dynamics.

This paper reviews an example of such architecture, composed by three dynamical systems in charge of generating the controls for a unicycle robot and a number of feedthrough maps that process the sensory information and shape the behavior of the dynamical systems. The novelty in the paper relies on the use of concepts from nonlinear analysis and control to validate the methodology.

A system of the type considered in this paper can be illustrated by the block diagram in figure 1, where block f_{robot} stands for a robot with configuration q, block $f_{\text{supervisor}}$ stands for a system that commands the robot and observing o from the environment, and block K just maps the outputs of f_{robot} into the inputs of $f_{\text{supervisor}}$. From a practical perspective, K can be thought of as the environment. In general, K is an arbitrary map with properties that make the analysis of the global system difficult so a neutrality argument is used ahead in the paper.

Dynamical systems have been widely used in robotics, [3], [14], [12], [9], [11], [4]. They are designed to be in or close to an attractor or to a limit cycle solution, and rapidly return to the attractor solution after transient perturbations of the state variables. The small number of configuration parameters tends to reduce the dimensionality of the control problem.

The paper briefly describes a dynamical systems based architecture and presents the analysis using concepts from nonlinear systems, namely on the existence of fixed points and on the use of the L_2 gain to measure stability. Simulation results using the Webots high fidelity simulation environment are presented at the end of the paper.

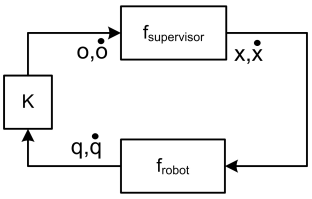

Figure 1. A graphical representation of the global system

II. A Dynamical Systems Based Architecture

The block diagram in figure 1 can be instantiated as in figure 2.

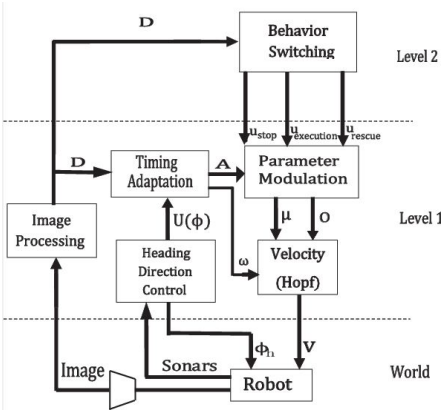

Figure 2. System overall schematic

The command system, $f_{\text{supervisor}}$, is composed by four subsystems (see [15]). The symbols $f_i, i = 1, \ldots, 10$, are used to identify each the equations with blocks in the architecture, simplifying the explanation ahead in the paper.

A Behavior Switching module, described by,

$$f_1 \triangleq \alpha_u \dot{u}_i = \beta_i u_i - |\beta_i| u_i^3 - \nu \sum_{a \neq i} u_a^2 u_i + \text{gwn}_u, \quad (1)$$

where $i = 1, 2, 3$ are just labels standing for three motor behaviors, *stop*, *execution*, and *rescue*. These different motor

behaviors will occur in response to specific stimulus and current states of the task at hand, expressed through logical conditions by a sigmoid function, controlling the competitive advantage parameters β_i. Parameter ν is chosen in order to destabilize any attractor in which more than one output u_i is "on ".

The output of the dynamics associated to each motor behavior are combined as,

$$f_2 \triangleq \; O_m = |u_1|O_s + |u_2|O_e + |u_3|O_r \tag{2}$$

$$f_3 \triangleq \; \mu = -\left(|u_1| + |u_3|\right)\frac{A^2}{2} + |u_2|A^2 \tag{3}$$

where $O_s = 0$, $O_e = A$, and $O_r = 0.1$.

Expressions (2,3) constitute the *Parameter Modulation* module which provides changes in values of the dynamical parameters of a modified Landau-Stuart oscillator of the *Velocity* module,

$$f_4 \triangleq \dot{m} = \alpha\left(\mu - \left((m-O_m)^2 + n^2\right)\right)(m - O_m) - \omega n \tag{4}$$

$$f_5 \triangleq \; \dot{n} = \alpha\left(\mu - \left((m-O_m)^2 + n^2\right)\right)n + \omega(m - O_m) \tag{5}$$

where ω specifies the oscillations frequency (rads^{-1}) and O_m is used to control the m solution offset. μ controls the type of stable solution that is achieved (fixed point $(m, n) = (O_m, 0)$ when $\mu < 0$ and stable oscillation when $\mu > 0$). Additionally, for $\mu > 0$, μ also encodes the amplitude of the rhythmic activity. The robot linear velocity is chosen as $v_{\text{robot}} = m$.

Considering the task of reaching a target, the required velocity profile is further subdivided into three time intervals, each one with different durations, such their sum equals the movement time $MT = T_1 + T_2 + T_3$. For $t \leq t_1$, the oscillator covers the first quarter of the limit cycle (T_1), half of the limit cycle is covered for $t_1 < t \leq t_2$ (T_2), and the last quarter is covered from $t_2 < t \leq t_3$ (T_3).

For each of the three time intervals the angular frequency ω in (4) is such that in the overall they are performed within the correct timing, as $\omega_1 = \frac{\pi}{2T_1}$, $\omega_2 = \frac{\pi}{T_2}$, $\omega_3 = \frac{\pi}{2T_3}$.

An updating rule for the Hopf radius cycle A, considering the current distance to the target, $D(t)$ and the remaining time to cover it, is given by,

$$A_1 = \frac{D\left(t\right)}{\frac{\frac{\pi}{2}-1+\sin(\omega_1 t)}{\omega_1} + \frac{\pi+2}{\omega_2} + \frac{\frac{\pi}{2}-1}{\omega_3} - t}, \;\; 0 < t \leq t_1 \tag{6}$$

$$A_2 = \frac{D\left(t\right)}{\frac{\frac{\pi}{2}}{\omega_1} + \frac{\pi+1+\cos(\omega_2(t-T_1))}{\omega_2} + \frac{\frac{\pi}{2}-1}{\omega_3} - t}, \;\; t_1 < t \leq t_2 \tag{7}$$

$$A_3 = \frac{D\left(t\right)}{\frac{\frac{\pi}{2}}{\omega_1} + \frac{\pi}{\omega_2} + \frac{\frac{\pi}{2}-\cos(\omega_3(t-T_1-T_2))}{\omega_3} - t}, \;\; t_2 < t \leq t_3 \tag{8}$$

The velocity profile is modulated in amplitude and frequency in the *Timing Adaptation* module, by modifying both A and ω parameters, respectively. These parameters are changed according to the oscillator current state as,

$$\mathrm{A}' = \frac{A_1}{\left(1 + \mathrm{e}^{b(m-O_m)}\right)\left(1 + \mathrm{e}^{bn}\right)} + \frac{A_2}{1 + \mathrm{e}^{-b(m-O_m)}} + \frac{A_3}{\left(1 + \mathrm{e}^{b(m-O_m)}\right)\left(1 + \mathrm{e}^{-bn}\right)}, \tag{9}$$

where A_1, A_2 and A_3 are as defined in equations (6),(7),(8), respectively and $b = 500$. The value of A' alternates between these three different values, A_1, A_2 and A_3, depending on the current values of m and n variables.

The same procedure is used for the ω parameter as follows,

$$f_9 \triangleq \; \omega \;\; = \;\; \frac{\omega_1}{\left(1 + \mathrm{e}^{b(m-O_{\mathrm{m}})}\right)\left(1 + \mathrm{e}^{bn}\right)} + \frac{\omega_2}{1 + \mathrm{e}^{-b(m-O_{\mathrm{m}})}} + \frac{\omega_3}{\left(1 + \mathrm{e}^{b(m-O_{\mathrm{m}})}\right)\left(1 + \mathrm{e}^{-bn}\right)} \tag{10}$$

The presence of obstacles is indicated by a potential function, $U(\phi_{\mathrm{h}})$ (see expression (14) ahead). The distance to obstacles, d_i, is measured by seven sonar sensors ($i = 1, ..., n_s, n_s = 7$) mounted on a ring centered on the robot's axis. If $U(\phi_{\mathrm{h}}) < 0$, the repulsion from obstacles contribution is weak for the current heading direction value; if $U(\phi_{\mathrm{h}}) > 0$, the current heading direction ϕ_h, is on a repulsion zone of sufficient strength and the robot must change its heading direction in order to avoid the obstacle. In this situation the velocity should decrease by reducing A. This is achieved by setting the A amplitude as follows,

$$f_{10} \triangleq \; A = A'\left(1 - \frac{1 - \min(d_i)/R}{1 + e^{-b(U(\phi_h)-1/b)}}\right) \tag{11}$$

where R is the maximum distance that the sonar sensors may detect (0.6 m).

The angular velocity of the robot, $\omega_{\text{robot}} = \dot{\phi}_h$, is generated in the *Heading Direction Control* module by,

$$f_7 \triangleq \quad \dot{\phi}_h \;\; = \sum_{i=1}^{n_s}\left(-\lambda_{obs,i}\left(\phi_h - \psi_i\right)e^{-\left(\frac{(\phi_h-\psi_i)^2}{2\sigma_i^2}\right)}\right) - \lambda_{target}\sin\left(\phi_h - \phi_{target}\right) + \mathrm{gwn}_{\phi} \tag{12}$$

$$f_6 \triangleq \quad \sigma_i \;\; = \tan^{-1}\left(\tan\left(\frac{\Delta\theta}{2}\right) + \frac{R_{robot}}{R_{robot} + d_i\left(t\right)}\right) \tag{13}$$

where $\Delta\theta$ is the sensor angular resolution, R_{robot} is the radius of the robot, d_i is the distance to obstacle detected by sensor i and n_s is the number of sensors. The orientation towards the target is represented by an attractive force erected at the direction ϕ_{target}. Repulsive forces created by each sonar are indicated by ψ_i and $-\left(\phi_h - \psi_i\right)$ corresponds to the sonar angular resolution, $\Delta\theta$. λ_{tar} ($\lambda_{\text{obs,i}}$) define the strength attraction (repulsion) that the target (repellor) exerts on the robot. $\lambda_{\text{obs,i}}$ is also dependent on d_i by $\left(\beta_1 \exp\frac{d_i}{\beta_2}\right)$, where β_1 and β_2 are positive constants.

The potential function indicating the presence of obstacles is obtained by integrating the obstacle force-lets and results in (see [2], [14]),

$$f_8 \triangleq U(\phi_h) = \sum_{i=1}^{n_s} \left(-\lambda_i \sigma_i^2 \exp\left[-\frac{(\phi_h - \psi_i)^2}{\sigma_i^2} \right] - \lambda_i \sigma_i^2 / \sqrt{e} \right) \tag{14}$$

III. A Nonlinear Systems Viewpoint

A mission can be defined as *successfully completed* under a number of alternatives, namely, (i) by reaching a point in the state space and staying there, (ii) by reaching a neighborhood of a point in the state space and staying there, and (iii) by reaching a point or a neighborhood and returning there, in finite time, infinitely many times. In this paper the analysis is restricted to the cases (i) and (ii), which require the existence of fixed points. Case (iii) includes the situations where the overall system reaches a limit cycle.

Proposition 1 (Mission success): A mission is completed successfully if the maps in figure 1 converge to a fixed point of the open loop maps[1] $f_{\text{robot}} \circ f_{\text{supervisor}}$ and $f_{\text{supervisor}} \circ f_{\text{robot}}$, and the fixed point is in the null space of the environment map K.

□

For the whole procedure to converge it is sufficient that $f_{\text{robot}} \circ f_{\text{supervisor}}$ and $f_{\text{supervisor}} \circ f_{\text{robot}}$ both have fixed points, that is if the composed maps are contracting. A weaker version requires that they are only non-expanding (see [5]).

Let $y = f_{\text{supervisor}}(x)$ and $x = f_{\text{robot}}(y)$. If $f_{\text{supervisor}} \circ f_{\text{robot}}$ is contracting the corresponding matrix of partial derivatives verifies $\|D(f_{\text{supervisor}} \circ f_{\text{robot}})\| < 1$. If the domain is convex then this condition means that the fixed point is unique (see Theorem 2.2.16 in [7]). Otherwise, the result holds only in a neighborhood of the fixed point.

Assuming the boundedness of each of the operators, applying the rule for differentiating a composed map yields,

$$\|D(f_{supervisor} \circ f_{robot})\| \leq \leq c \, \|Df_{supervisor}\| \cdot \|Df_{robot}\| \tag{15}$$

for some constant c. This means that for a generic robot, for which there is no information on the structure of f_{robot}, one must instead ensure that $\|Df_{\text{supervisor}}\| << 1$ which will be sufficient for the existence of a fixed point, independently of the model of the robot[2].

However, if instead of having a composed map that is contracting a weaker non-expanding property is obtained then theorem 2.4.4 in [5] ensures that a fixed point exists provided that the domain of the map is convex.

A similar reasoning can be made for the second composed map. Note that the requirement for this second map to have also a fixed point results directly from an argument similar to (15).

[1] We denote by $\circ$ the composition operation.

[2] A common matrix norm is defined as $\|A\| = \max_{x \neq 0} \frac{\|A(x)\|}{\|x\|} = \max_{\|x\|=1} \|A(x)\|$, with $x \in \mathbb{R}^n$ and $\|x\|$ the vector norm induced by the inner product.

The requirement that the fixed point is in the null space of the map K does not imply any lack of generality. In practical terms it simply means that the environment is neutral and the perception of the state of the robot is not changed. In case the neutrality does not hold the environment can be modeled as a composition of a "neutral map" with a "non-neutral" map, which must then be included in the composition of $f_{\text{supervisor}}$ and f_{robot}.

■

In general the uniqueness of the domain can not be guaranteed and hence the proposition above holds only in a neighborhood of the mission target. In a sense, this approach is equivalent to the small-gain theorem common in control theory (see theorem 5.6. in [10]).

The mesh of maps can be better visualized as the block diagram in figure 3a. A two step simplification of the full block diagram is shown in figures 3b and 3c. Rectangular shapes indicate dynamical systems whereas triangle shapes represent direct feedthrough maps.

It is easy to verify that each of the f_i maps is C^1 which somewhat simplifies the analysis. Also, it is worth to remark that the block meshes include both direct feedthrough and differential maps. The general idea that supports the analysis of the whole mesh is to analyze differential maps following the contraction mapping theorem and using the direct feedthrough maps as scaling transformations.

A. Temporally unconstrained singleton goal missions

Even though a generic robotic system is usually better modeled by a hybrid system, with the state evolution regulated both by continuous/discrete time and by events, in a wide variety of robotic systems imposing a smoothness constraint does not imply a significant loss of generality.

In the aforementioned first scenario a mission is successful when the whole system reaches a fixed point. Conditions for the existence of fixed points in C^1 dynamic systems are well known (see for instance [7]).

The (f_4, f_5) block represents the core dynamic system responsible by the generation of timed trajectories according to established temporal constraints, whereas the block (f_3, f_9, f_{10}), is a direct feedthrough map (as it contains no internal feedback loops). The two form a closed loop dynamic system (see figure 3b). Blocks (f_1, f_2) and (f_6, f_7, f_8) are also feedthrough maps that provide serial inputs to this loop. The whole f_i blocks form the robot supervisor. From figure 3c, this supervisor is a serial composition of $(f_2, f_4, f_5, f_3, f_9, f_{10})$ with f_1 and (f_6, f_7, f_8). The condition for the robot to complete successfully its mission is that the loop formed with (f_{robot}, K) has a fixed point at the target. Following the argument in section II, we assume that K is neutral and has no influence on the output of f_{robot}, that is K is the identity map.

Though it is easy to verify that, by construction, (1)-(14) has indeed a fixed point at the target, it remains to demonstrate that

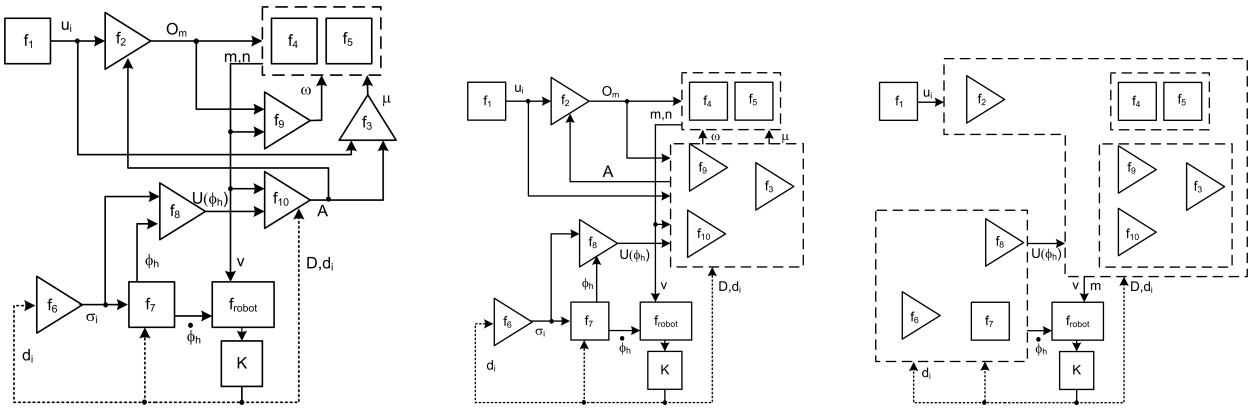

(a) Full version (b) After simplification stage 1 (c) After simplification stage 2

Figure 3. Block mesh representing the complete system

the contracting map conditions hold to ensure that the whole system is stable.

The conditions for the stability of (f_4, f_5) can be easily verified. A sufficient condition is that $\|D(f_4, f_5)\| < 1$, where $D(f_4, f_5)$ is the matrix of partial derivatives, in a neighbourhood of the fixed point (see for instance Theorem 2.2.16 in [7]).

Using the 2-norm for a matrix A defined as $\|A\|_2 = \max_{\|x\|_2=1} \|Ax\|_2 = \rho(A'A)$, with $\rho(A'A)$ the spectral radius of $A'A$ corresponds to a worst case scenario (since for any matrix norm $\|A'A\| \geq \rho(A'A)$ (see theorem 5.6.9. in [8]) and hence $\|A\| \geq \sqrt{\|A'A\|} \geq \sqrt{\rho(A'A)}$).

For the loop itself to verify the condition it is sufficient (but not necessary) that the block (f_3, f_9, f_{10}) have $\|D(f_3, f_9, f_{10})\| < 1$.

An upper bound for $\|D(f_3, f_9, f_{10})\|$ can be obtained directly (as the blocks have no interconnections among themselves) by bounding the norms $\|D(f_3, f_{10})\|$ and $\|Df_9\|$. The former can be bounded as $\|D(f_3, f_{10})\| \leq \|Df_3\|\|f_{10}\|$, where in general $\|Df_3\|$ will be arbitrary (there is no parameter to control this term) and $\|Df_{10}\|$ can be made arbitrarily small by careful selection of the T_j. Using the ω_i and (10), if the time allowed for the mission, determined by the T_j, is arbitrarily large then $\|D(f_3, f_9, f_{10})\| < 1$. The later can also be easily bounded by adequate choice of the parameters T_j and b.

Once the block $(f_3, f_4, f_5, f_9, f_{10})$ is found to have a fixed point one can analyze the loop formed by $(f_2, f_3, f_4, f_5, f_9, f_{10})$. This loop is also stable as $\|D(f_2, f_3, f_4, f_5, f_9, f_{10})\| \leq \|D(f_3, f_4, f_5, f_9, f_{10})\|\|Df_2\|\|Df_{10}\|$ can be upper bounded below 1 (using parameters b, Tj) even though $\|Df_2\|$ can be arbitrary.

Block $(f_1, f_2, f_3, f_4, f_5, f_9, f_{10})$ is a series composition and hence $\|D(f_1, f_2, f_3, f_4, f_5, f_9, f_{10})\| \leq \|Df_1\|\|D(f_2, f_3, f_4, f_5, f_9, f_{10})\|$. By adequate choice of parameters α_u, β_i (f_1 has no external inputs and hence it acts on the remaining blocks as generating parameters u_i; see also the discussion in [6]) it is possible to make $\|D(f_1, f_2, f_3, f_4, f_5, f_9, f_{10})\| < 1$ and hence the whole block is stable.

Block (f_6, f_7) is a series composition that clearly has a fixed point for adequate choice of parameters $\lambda_{obs}, \lambda_{target}$ (which can make $\|Df_7\|$ arbitrarily small). However, note that this may correspond to relaxing the time for the robot to complete the mission and its compliance with obstacle collision.

The final composition involves the series composition of the blocks (f_6, f_7, f_8) with $(f_2, f_3, f_4, f_5, f_9, f_{10})$. Using the previous arguments and given that $D(f_8, f_6)$ can be made arbitrarily small by adequate choice of the λ_i parameters one concludes that $\|f_{supervisor}\|$ can be made arbitrarily small, eventually requiring the relaxation of the performance of the mission.

Extending the result to the whole system, including f_{robot} requires that $\|Df_1, f_2, f_3, f_4, f_5, f_9, f_{10}, f_{robot}\|$ and $\|Df_6, f_7, f_{robot}\|$ be smaller than 1. For the typical unicycle robot $\|Df_{robot}\| < \max\{1, v^2\}$, which means that $\|Df_1, f_2, f_3, f_4, f_5, f_9, f_{10}, f_{robot}\| < 1$ is a sufficient condition for $\|Df_6, f_7, f_{robot}\| < 1$ also. From the above arguments, one concludes that the unconstrained architecture can always be stabilized.

B. Temporally constrained singleton goal missions

In a sense, if a control architecture is able to reach a fixed point that corresponds to the mission target, then bounding the time it takes to reach the target (or an arbitrary small neighborhood around it) amounts to require that the system is fast enough. The purpose of this section is thus to use a global property such as the L_2 system gain to assess the capability of the system to fulfill a temporal constraint.

For the purpose of this paper, a temporal constraint is just an upper bound on the amount of time a system can take to reach a certain region in the state space. Without loosing generality, this region can be assumed to be a neighborhood of some target point.

Definition 1 (Temporal constraint): A dynamical system $\dot{q} = f(q, t, u)$ with initial condition q_0 verifies a temporal constraint if

$$\forall \epsilon > 0,\ \forall t_f, q_f, q_0,\ \exists u(t)\ :\ q(t) \in \mathcal{B}(q_f, \epsilon),\ t > t_f$$

where t is the time, u are the command inputs of the system, q_f stands for the desired final configuration, and t_f for the max allowed time for the mission.

□

Definition 1 reads as after t_f the state $q(t)$ is close enough to q_f, that is, at maximal distance ϵ, or the distance between $q(t_f)$ and q_f is at most ϵ.

Consider the index

$$J(t) = \int_{t_0}^{t} d\left(q(t), \mathcal{B}(q_f, \epsilon)\right) dt \tag{16}$$

where $d(,)$ is a distance operator, for instance a norm of the projection of $q(t)$ onto $\mathcal{B}$.

Taking the distance measure as the norm induced by the usual inner product in $\mathbb{R}^n$,

$$\begin{aligned} d(q(t), \mathcal{B}(q_f, \epsilon)) &= \|q_f - q\| - \epsilon \\ &= \|q_f\|^2 + \|q(t)\|^2 - \epsilon - 2\langle q(t), q_f \rangle \end{aligned}$$

where $\langle , \rangle$ stands for the inner product. The term $\langle q(t), q_f \rangle$ can always be made positive by adequate choice of the reference frame and hence

$$d(q(t), \mathcal{B}(q_f, \epsilon)) \leq \|q_f\|^2 + \|q(t)\|^2 - \epsilon \tag{17}$$

is a conservative upper bound for the distance.

The L_2 gain models the system from an input-output viewpoint. The global system that corresponds to the composition of $f_{supervisor}$ and f_{robot} has inputs $d_i, \psi_i, \phi_{target}, D$, and outputs the trajectory of the robot.

The L_2 gain of a system is the smallest γ constant such that a constant b exists and the following inequality holds, [13],

$$\int_0^t \|q(t)\|^2 dt \leq \gamma^2 \int_0^t \|u(t)\|^2 dt + b, \qquad \text{for all } t > 0 \tag{18}$$

Using (17) and (18) in (16) yields

$$J(t) \leq \int_{t_0}^{t} \left(\|q_f\|^2 - \epsilon\right) dt + \gamma^2 \int_{t_0}^{t} \|u(\tau)\|^2 d\tau + b \tag{19}$$

Assuming that the robot reaches the target, then $J(t)$ approaches a majorant $J_{\max}$ and by Lemma 8.2 in [10], $d(t) \to 0$. Therefore, the righthand side of (19), denoted $\overline{J}$, can also be hard limited without loosing generality (for example forcing $\|u(t)\| = 0$ as soon as the robot reaches the target). The bound $\overline{J}$ can be used to obtain conclusions on the L_2 gain, namely by identifying $V(t) = J_{\max} - \overline{J}(t)$ with a Lyapunov function. $-\dot{J}(t)$ is negative definite and using the generalized Lyapunov condition (see for instance [10], chapter 8, or [1], chapter 6, for more general systems)

$$\dot{V}(t) \leq -W(t) \tag{20}$$

with $W(t)$ a decreasing positive definite function.

Substituting $\dot{V}(t)$ by the bound on the righthand side of (19) yields

$$-\left(\|q_f\|^2 - \epsilon + \gamma^2 \|u(t)\|^2\right) \leq -W(t) \tag{21}$$

This does not imply any loss of generality. In fact, it corresponds to tightening the stability bound (20). To estimate the γ required for a timing constraint to be verified requires that assumptions on the decrease rates for $\|u\|^2$ and W be made. Assuming linear bounds,

$$\|u(t)\|^2 \leq m_u\, t + b_u \tag{22}$$

$$W(t) \leq m_W\, t + b_W \tag{22b}$$

for adequate m_u, b_u, m_W, b_W. These bounds represent the max control effort and the stability bound. Substituting in (21),

$$\gamma^2 \geq \frac{m_W\, t + b_W - \|q_f\|^2 + \epsilon}{m_u\, t + b_u}, \qquad \text{for all } t \tag{23}$$

Again, note that there is no loss of generality here. By using (22) one is being optimistic on the control effort required. Instead, using a lower bound in (22) would amount to a conservative estimate for the control effort.

Expression (23) yields a lower bound for the L_2 gain of the overall system under the assumptions that control is used accounting for (22) and that the stability bound $W(t)$ is not violated.

The righthand side of (23) can be put in a more suitable form by being conservative and using a majorant, that is,

$$\gamma^2 \geq \begin{cases} \frac{b_W + \|q_f\|^2 - \epsilon}{b_u} & \text{if } \|u\|^2 \leq W \\ \frac{m_W t_f + b_W}{m_u t_f + b_u} + \frac{\|q_f\|^2 - \epsilon}{b_u} & \text{otherwise} \end{cases}$$

The above considerations suggest that the L_2 gain is a consistent measure of the system capability to fulfill the temporal constraint.

It is worth to point that the analysis in this section is compatible with a broader hybrid systems perspective. In fact, if some of the blocks in the architecture are of hybrid type, e.g., changing its structure according to some events, the generalized Lyapunov condition (20), with the lefthand side replaced by adequate generalized derivative such as Dini's upper contingent derivative, still applies. The role of the L_2 gain on the stability of switched systems (a less general class of hybrid systems) has been discussed, for example, in [16].

IV. Experiments

This section presents a set of experiments that illustrate the ideas of the previous sections. As mentioned in the initial section, a synthetic Webots environment is used as it simplifies the replication of experiments in controlled conditions. The Webots environment is widely used in robotics for its fidelity emulating kinematics and dynamics of a wide range of commercial robots such as the Pioneer AT used in this work.

The first experiment (figure 4a) illustrates how the conditions for the existence of a fixed point hold during a mission in which there are no obstacles. A unicycle Pioneer

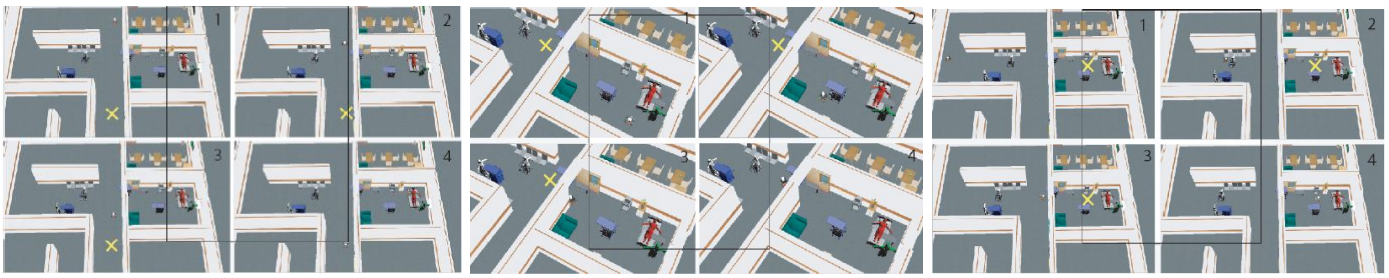

(a) Exp 1 - No obstacles (b) Exp 2 - Easy obstacles (c) Exp 3 - Static and dynamic obstacles

Figure 4. Experiments

AT robot must travel a 5m long path in 30s. The robot completes the mission successfully. The max singular value of $Df'_{supervisor}Df_{supervisor}$ matrix, corresponding to the 2-norm of matrix $\|Df_{supervisor}\|$ never exceeds 0.016, in agreement with Proposition 1.

The second experiment (fig 4b includes two obstacles and the robot has to cover around 7.5m in 50s. As before $\|Df_{supervisor}\| < 1$ during the whole mission (the max singular value is always below 2.2×10^{-6}).

In the third experiment (figure 4c) the robot has to cover around 14m in 30s while avoiding static obstacles and a dynamic obstacle moving at 0.2m/s. As before $\|Df_{supervisor}\| < 1$ during the whole mission (the max singular value always below 2.3×10^{-7}).

Table I shows the L_2 bounds for the global system. The L_2 gain lower bound from (23) is denoted $\underline{\gamma}$. Note that negative values for $\underline{\gamma^2}$ simply reflect the fact that the linear bound $W(t)$ approach the horizontal line and hence (23) is verified for all t.

Exp.	γ	$\underline{\gamma^2}$	m_W	b_W	m_u	b_u
1	3.320	-0.043	-0.0071	-0.225	-24.738	776.764
2	3.320	0.827	0.0023	-0.117	-201.411	6324.324
3	3.320	0.828	0	0	-201.412	6324.324

Table I
L_2 LOWER BOUND

For all experiments, the L_2 estimate is bigger than the lower bound identified in (23), in accordance with the results in section III-B.

V. CONCLUSIONS

The paper presents a nonlinear systems viewpoint for a well known robot control architecture. Mission targets are identified with the fixed points of the overall dynamic system and the L_2 gain was shown to describe a system property suitable to represent the ability of the system to account for timing constraints. This is an interesting aspect that can be extended to other architectures, i.e., the L_2 gain of a robot control architecture is a measure of its ability to cope with temporal constraints.

Webots based experiments were presented to illustrate the analysis. Future work includes the development and experiments when target is a goal region instead of a single point.

ACKNOWLEDGMENTS

This work was partially supported by FCT projects PEst-OE/EEI/LA0009/2011 and PTDC/EEA-CRO/100655/2008, and grant SFRH/BD/68805/2010.

REFERENCES

[1] J.P. Aubin and A. Cellina. *Differential Inclusions*. Springer-Verlag, 1984.
[2] E. Bicho, P. Mallet, and G. Schöner. Target representation on an autonomous vehicle with low-level sensors. *The International Journal of Robotics Research*, (210), 2000.
[3] R. Blickhan. The spring-mass model for running and hopping. *Journal of Biomechanics*, 22(11-12):1217–1227, 1989.
[4] Luiz Castro, Cristina Santos, Miguel Oliveira, and Auke Ijspeert. Postural Control on a Quadruped Robot Using Lateral Tilt: A Dynamical System Approach. In *EUROS*, volume 44 of *Springer Tracts in Advanced Robotics*, pages 205–214. Springer, 2008.
[5] Kung-Ching Chang. *Methods in Nonlinear Analysis*. Springer Monographs in Mathematics. Springer, 2005.
[6] H. I. Christensen E. Large and R. Bajcy. Scaling the dynamic approach to path planning and control: Competition amoung behavioral constraints. *The International Journal of Robotics Research*, (18):37–58, 1999.
[7] Boris Hasselblatt and Anatole Katok. *A First Course in Dynamics*. Cambridge University Press, 2003.
[8] Roger A. Horn and Charles R. Johnson. *Matrix Analysis*. Cambridge University Press, 21 edition, 2007. First published, 1985.
[9] Auke Jan Ijspeert, Jun Nakanishi, and Stefan Schaal. Learning Attractor Landscapes for Learning Motor Primitives. In *Advances in Neural Information Processing Systems 15*, pages 1547–1554. MIT Press, 2002.
[10] W. Khalil. *Nonlinear Systems*. Prentice Hall, 2002.
[11] C. P. Santos. Generating Timed Trajectories for an Autonomous Vehicle: A Non-linear Dynamical Systems Approach. In *IEEE International Conference on Robotics and Automation (ICRA-2004)*, 2004.
[12] S. Schaal, S. Kotosaka, and D. Sternad. Nonlinear dynamical systems as movement primitives. In *First IEEE/RAS International Conference on Humaniod Robotics (Humanoids 2000*, 2000.
[13] Arjan van der Schaft. *L_2-Gain and Passivity Techniques in Nonlinear Control*. Springer, 2000.
[14] G. Schöner and M. Dose. A dynamical systems approach to task-level system integration used to plan and control autonomous vehicle motion. *Robotics and Autonomous Systems*, 10(4):253–267, 1992.
[15] J. Silva, C. Santos, and V. Matos. Timed Trajectory Generation for a Toy-like Wheeled Robot. *36th Annual Conference of the IEEE Industrial Electronics Society, Glendale, USA, November 07-10*, pages 1645–1650, 2010.
[16] Jun Zhao and David J. Hill. On Stability and L_2-gain for Switched Systems. In *Procs. of the 44th IEEE Conf. on Decision and Control and European Control Conference*, December 2005. Seville, Spain.